Raman scattering from in-plane lattice modes in low-stage graphite–alkali-metal compounds*

P. C. Eklund,† G. Dresselhaus,‡ and M. S. Dresselhaus†
Massachusetts Institute of Technology, Cambridge, Massachusetts 02139

J. E. Fischer§
University of Pennsylvania, Philadelphia, Pennsylvania 19104

(Received 7 April 1977)

Low-temperature Raman scattering results for stage 1, 2, and 3 graphite–alkali-metal intercalation compounds are reported for in-plane modes using the Brewster-angle back-scattering geometry. Detailed full spectra are presented for stage 1, 2, and 3 compounds of graphite-Rb at 77 K. Particular attention is given to the structure which occurs at $\gtrsim 560$ cm^{-1} in the stage-1 compounds C_8K, C_8Rb, C_8Cs. This structure is shown to have two components of different symmetries and is related to the zone-edge M_{1g} phonon mode of pristine graphite.

Of the various classes of graphite intercalation compounds, the alkali-metal compounds are the simplest insofar as the intercalate species is atomic (or ionic) rather than molecular. The objective of this paper is (a) to present Raman scattering results for graphite-Rb (Fig. 1), (b) to emphasize a commonality in the lattice properties of the three alkali-metal compounds, (graphite-K, graphite-Rb, and graphite-Cs which also have closely related electronic[1] and structural properties,[2,3]), and (c) to relate the Raman spectra in these intercalation compounds to lattice modes in pristine graphite.[4,5]

The Raman spectra of Fig. 1 were taken on c faces of stage-1 (C_8Rb), stage-2 ($C_{24}Rb$), and stage-3 ($C_{36}Rb$) compounds[1] using the Brewster-angle backscattering geometry. The spectra therefore correspond to the excitation of in-plane Raman modes. To avoid intercalate desorption effects associated with laser heating, these spectra were taken at 77 K using low laser power levels and cylindrical laser focusing.

A comparison of spectra for graphite-Rb with those published by Nemanich, Solin, and Guerard[6] for graphite-K and graphite-Cs reveals two important points. A qualitatively different spectrum is observed for each of the three lowest stages n, $n=1$, 2, 3. However, for each of these stages n, the spectra for the three intercalate species K, Rb, and Cs are very similar. One objective of this paper is to expand on these two points.

The spectra for the stage-3 alkali-metal compounds exhibit a doublet structure (e.g., for $C_{36}Rb$ the doublet components are at 1579 cm^{-1} and 1605 cm^{-1}) which is also observed in a variety of graphite-acceptor intercalation compounds for stage $n>2$.[6,7] Both components of this doublet structure are identified with carbon-atom lattice modes for the following two reasons. First, the spectra for the various compounds show the frequencies of the doublet to lie close to the E_{2g_2} mode of pristine graphite[4] and to be essentially independent of intercalate species and of intercalate concentration x.[6,7] Secondly, the intensity of the component close to the E_{2g_2} Raman-active mode for pristine graphite *decreases* with increasing x, while the intensity of the up-shifted line *increases* with increasing x. The lower and upper frequency components are, respectively, identified with carbon-atom vibrations in planes *not adjacent* to and planes *adjacent* to an intercalate layer plane. Consistent with this interpretation, Fig. 1 shows that the intensity of the lower frequency line at 1579 cm^{-1} decreases (and perhaps disappears) in going from a stage-3 to a stage-2 compound, in agreement with the spectra reported for $C_{24}K$ and $C_{24}Cs$ and the observation that for stage-2 compounds, all graphite planes are adjacent to inter-

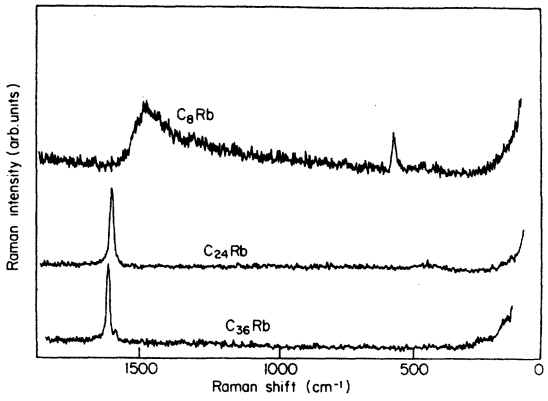

FIG. 1. Raman spectra of C_8Rb (stage 1), $C_{24}Rb$ (stage 2), and $C_{36}Rb$ (stage 3). The data were taken in the Brewster-angle backscattering geometry at 77 K. The line-shape parameters are given in Table I.

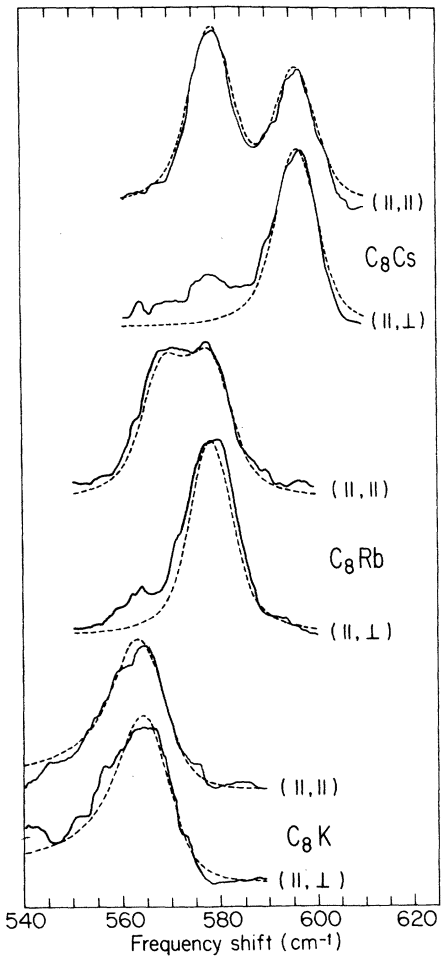

FIG. 2. Raman scattering intensity at 77 K for stage-1 alkali-metal compounds C_8K, C_8Rb, and C_8Cs in the region of 560 cm^{-1} using the Brewster-angle backscattering geometry for incident and scattered light propagating in the $z,\bar{z}$ directions, respectively. The polarization directions for incident and scattered light are indicated. The polarization effects observed for the $(\|,\|)$ and $(\|,\perp)$ polarization geometries are consistent with the identification of the observed structures with the M_{1g} mode for pristine graphite folded back to $\vec{k}=0$ in the intercalation compound. The upper-frequency component of the observed structure is identified with E_{2g} symmetry and the lower-frequency component with A_{1g} symmetry. The dashed curves are a fit to the data using the parameters given in Table I, and appropriate corrections for the instrument function.

calate planes.[6,7] These results further indicate that it is the lattice modes derived from the Γ-point E_{2g_2} mode of pristine graphite (rather than for example, a zone-edge mode which is folded into the Γ point because of the larger real-space unit cell of the intercalation compound) which dominate these spectra because of the proximity of the Raman frequencies in these intercalation compounds to the E_{2g_2} mode in pristine graphite.

On the other hand, the spectra for the first stage C_8K, C_8Cs, and C_8Rb compounds are very similar to each other, but very different from the spectra for the higher-stage compounds. Characteristic of the spectra for the three stage-1 alkali-metal intercalation compounds is a high-frequency feature (≈ 1500 cm^{-1}) and an intermediate frequency feature ($\gtrsim 560$ cm^{-1}), which is shown in more detail in Fig. 2; this intermediate frequency feature is absent in the spectra for the higher-stage intercalation compounds. We attribute both features to carbon-atom vibrations because of their relative insensitivity to intercalate species. In this connection, we further note that the intermediate frequency feature is upshifted in frequency as the mass of the intercalate species increases (see Table I), contrary to what would be expected if the intermediate frequency feature were associated with an intercalate mode.

For the three compounds C_8K, C_8Rb, and C_8Cs, the broad line ≈ 1500 cm^{-1} has an asymmetrical Breit-Wigner line shape[8] with a frequency-dependent scattering intensity $I(\omega)$ given by

$$I(\omega)=I_0\left[1+\left(\frac{\omega-\omega_0}{q\Gamma}\right)\right]^2 \Big/ \left[1+\left(\frac{\omega-\omega_0}{\Gamma}\right)^2\right],$$

in which I_0 is a normalization factor for the scattering intensity, ω_0 is the resonant frequency corresponding to intensity I_0, Γ is a measure of the linewidth, and q^{-1} is the Breit-Wigner coupling coefficient. As $q^{-1}\to 0$, a Lorentzian line shape results. A partial listing for the Breit-Wigner parameters at temperatures of 300, 77, and 4 K is given in Table I for stage $n=1,2,3$ alkali-metal compounds. In this listing, a negative (positive) sign for q indicates that the strongest coupling is to a continuum of *lower-* (higher-) frequency states. It is seen that the Breit-Wigner parameters change significantly between room temperature and 77 K, but are almost constant between 77 and 4 K. The room-temperature entries in this table are taken from Ref. 6. We attribute the large linewidth of the line ≈ 1500 cm^{-1} to mode coupling to a continuum of states arising from both in-plane and c-axis zone folding effects. For stage-1 compounds, there are no longer inequivalent planar A and B carbon-atom sites.[1,2] Thus, the distinction between E_g and E_u graphite modes is no longer relevant and Raman-active modes can result from zone folding effects for zone-edge modes such as the M_{2u} and M_{4u} modes,[8] which are folded into the Γ point in the smaller Brillouin zone for the C_8X intercalation compounds. The modes arising from in-plane zone folding effects may not be individually resolved because of concomitant c-axis zone folding effects due to differences in site occupation

TABLE I. Raman line-shape parameters of graphite–alkali-metal intercalation compounds.

Material	Stage	T (K)	ω_0	Γ	Γ/q	Polarization [b]
Graphite [a]	∞	300	1582	7	0	none
$C_{36}Rb$	3	77	1605 ±1	5 ±0.5	0.6 ±0.2	none
		77	1579 ±1	6 ±0.5	0 ±0.2	none
$C_{24}Rb$	2	77	1602 ±1	7 ±0.5	0.6 ±0.2	none
C_8Rb	1	77	1480 ±10	60 ±5	−18 ±1	none
		77	576 ±1	5 ±0.5	−1.8 ±0.1	none
		77	569 ±0.5	3.5 ±0.5	0 [b]	(∥,∥)
		77	578.5 ±0.5	3.0 ±0.5	0 [b]	(∥,∥),(∥,⊥)
		4	1490	50	−14	none
$C_{36}Cs$	3	300 [c]	1604	~9	···	none
		300 [c]	1579	~5	···	none
$C_{24}Cs$	2	300 [c]	1598	~22	···	none
C_8Cs	1	300 [c]	1519	95.6	−95.6	none
		300 [c]	558 [d]	9.7	−3.9	none
		77	1520	25.0	−10	(∥,∥),(∥,⊥)
		77	579 ±0.5	2.5 ±0.5	0 [b]	(∥,∥)
		77	596 ±0.5	2.0 ±0.5	0 [b]	(∥,∥),(∥,⊥)
		4	1515	25	−9	none
$C_{24}K$	2	300 [c]	1599	13	···	none
C_8K	1	300 [c]	1547	78.7	−98.4	none
		300 [c]	566	9.1	−4.3	none
		77	565.4 ±0.5	5 ±0.5	−1 ±0.2	(∥,∥)
		77	566.0 ±0.5	5 ±0.5	−1 ±0.2	(∥,⊥)

[a] Spectra are at room temperature (Ref. 4). The line shapes here are Lorentzian.

[b] Correction for the instrument function is included only in the analysis of the polarized data. The analysis for C_8Cs and C_8Rb assumes Lorentzian line shapes ($\Gamma/q=0$) and for the unresolved doublet in C_8K a Breit-Wigner line shape was used. However, the displacement of the base line suggests that at least one of the lines (E_{2g} component) has a sizeable Breit-Wigner parameter $\Gamma/q \cong 0.5$. In the table "none" indicates no polarization analysis was made.

[c] The room-temperature data in this table are from Ref. 6. In this reference, the authors recognized that the line shapes for the stage-2 and -3 compounds possessed the characteristic Breit-Wigner asymmetry but used a Lorentzian line-shape analysis for simplicity for these higher-stage compounds. The linewidths given here represent our estimates based on the traces shown in Ref. 6.

[d] This value is from room-temperature data of Ref. 6. No doublet structure was reported by these authors.

in the intercalate layers, as for example the α, β, γ, δ stacking of intercalate layers in C_8K.[1,2] Intercalation causes a lowering of the symmetry of the pristine graphite and introduces a much larger number of Raman-active modes as well as a greater number of interacting modes with similar symmetry. If the perturbation interaction between the graphite and alkali-metal layers is sufficiently strong, a large number of Raman-active modes spanning the frequencies of the upper optical modes (see Ref. 5) can participate in the Raman process and a density-of-states model for unresolved modes results. A strong interaction between the intercalate and graphite planes is also consistent with results of Knight shift[9] and Mössbauer[10] studies, showing a large charge transfer between the alkali-metal and graphite layers. Because the alkali-metal modes are very soft, the magnitude of the frequency upshift due to the graphite-intercalate interaction is expected to be small.

In Fig. 2, we show in more detail the feature in the Raman spectra in the 560-cm^{-1} region using polarized light (see Fig. 1 for C_8Rb). The spectra in Fig. 2 for C_8K, C_8Rb, and C_8Cs are all obtained at low (77 K) temperature. We denote by z and $\bar{z}$ the propagation directions of the incident and scattered light in the backscattering geometry. The polarization directions are further indicated in Fig. 2 in parentheses for the direction of the

electric field for the incident and scattered beams. Thus (||, ||) refers to the $z(x,x)\bar{z}$ or $z(y,y)\bar{z}$ scattering geometries, while (||, ⊥) refers to the $z(x,y)\bar{z}$ or $z(y,x)\bar{z}$ scattering geometries. Our symmetry analysis shows the structure in the vicinity of ≈560 cm^{-1} to contain two components. The peak frequencies for the two components of the structure are given in Table I for each trace of Fig. 2, fitting each component to a Lorentzian line shape for the case of C_8Cs and C_8Rb as shown by the dashed curves in the figure. For C_8K, the structure in Fig. 2 appears as an unresolved asymmetric structure which was fit by a Breit-Wigner line shape (dashed curve) using the parameters given in Table I. [In carrying out the analysis in Fig. 2, the Breit-Wigner expression of Eq. (1) is convoluted with the instrument function.]

The largest splitting between the components is observed in C_8Cs and hence the clearest symmetry assignment can be made in this case. We identify the lower-frequency component with A_{1g} symmetry and the upper-frequency component with E_{2g} symmetry, corresponding to the folding of the three equivalent zone-edge graphitic M_{1g} modes (see Fig. 8 of Ref. 5) into the Γ point of the smaller C_8X Brillouin zone. For C_8Cs, the doublet is observed in the (||, ||) polarization geometry (where both A_{1g} and E_{2g} are symmetry-allowed), but only a single line occurs for the (||, ⊥) polarization (where only E_{2g} is symmetry-allowed). For the case of C_8Rb, evidence for the doublet structure comes from the much smaller linewidth observed for the (||, ⊥) polarization as compared with the (||, ||) linewidth. The doublet structure is not resolved for C_8K. The doublet structure in Fig. 2 is split by a frequency $\Delta\omega$ and the "center of gravity" of the doublet is up-shifted by $\delta\omega$ from the M_{1g} mode in pristine graphite. Both $\Delta\omega$ and $\delta\omega$ are attributed to an interaction between the graphite and intercalate layers. If the ratio $(\Delta\omega/\delta\omega)$ is assumed to be the same for C_8Cs, C_8Rb, and C_8K then the splitting $\Delta\omega$ follows the sequence (≈1, 9, 17) for the K, Rb, and Cs compounds, respectively, and places the M_{1g} level for pristine graphite at 560 cm^{-1}. This interpretation of the doublet structure requires the M_{1g} level for pristine graphite to lie lower than is given by the analysis in Ref. 5.

This identification of the various structures, observed in the Raman spectra of the alkali-metal compounds, with phonons derived from lattice modes for pristine graphite, accounts for the similarity of the K, Rb, and Cs spectra for a given stage compound. We attribute the dependence of the observed spectra on the stage of the compound ($n=1$, 2, and 3) to a difference in lattice symmetry for these stages. A detailed analysis of the lattice symmetry for C_6X, C_8X, $C_{18}X_2$, and $C_{24}X_2$ compounds is presented in a forthcoming publication.[11]

ACKNOWLEDGMENTS

We wish to thank Dr. D. D. L. Chung for valuable discussions and Professor S. A. Solin for making available to us a preliminary unpublished version of Ref. 6.

*Work supported in its initial phases under NSF Grant No. DMR 76-12226 and later under ONR Grant No. N00014-77-C-0053.

†Department of Electrical Engineering and Computer Science and Center for Materials Science and Engineering. Visiting Scientists, Francis Bitter National Magnet Laboratory.

‡Francis Bitter National Magnet Laboratory, supported by the National Science Foundation.

§Moore School of Electrical Engineering and Laboratory for Research on the Structure of Matter. The sample preparation was carried out under support from the National Science Foundation MRL Program, Grant No. DMR-76-00678.

[1]L. C. F. Blackman, J. F. Mathews, and A. R. Ubbelohde, Proc. R. Soc. A 258, 339 (1960).

[2]D. E. Nixon and G. S. Parry, Brit. J. Appl. Phys. 1, 291 (1968).

[3]G. S. Parry, in *Proceedings of the Third Conference in Industrial Carbon and Graphite* (Society of Industrial Chemistry, London, 1971), p. 58.

[4]L. J. Brillson, E. Burstein, A. A. Maradudin, and T. Stark, in *Proceedings of the International Conference on the Physics of Semimetals and Narrow Gap Semiconductors, Dallas, Texas, 1970,* edited by E. L. Carter and R. T. Bate (Pergamon, New York, 1971), p. 187.

[5]R. Nicklow, N. Wakabayashi, and H. G. Smith, Phys. Rev. B 5, 4951 (1972).

[6]R. J. Nemanich, S. A. Solin, and D. Guerard, Phys. Rev. B (to be published).

[7]J. J. Song, D. D. L. Chung, P. C. Eklund, and M. S. Dresselhaus, Solid State Commun. 20, 1111 (1976).

[8]J. F. Scott, Rev. Mod. Phys. 46, 83 (1974).

[9]G. P. Carver, Phys. Rev. B 2, 2284 (1970).

[10]L. E. Campbell, G. L. Montet, and G. J. Perlow, Phys. Rev. B 15, 3318 (1977).

[11]G. Dresselhaus, M. S. Dresselhaus, and P. C. Eklund, (unpublished).